Dual role for the methyltransferase G9a in the maintenance of β-globin gene transcription in adult erythroid cells

Chandra-Prakash Chaturvedi[a,1], Alison M. Hosey[a,1], Carmen Palii[a], Carolina Perez-Iratxeta[a], Yoshihiro Nakatani[b], Jeffrey A. Ranish[c], F. Jeffrey Dilworth[a,d], and Marjorie Brand[a,d,2]

[a]The Sprott Center for Stem Cell Research, Regenerative Medicine Program, Ottawa Hospital Research Institute, Ottawa, ON Canada K1H 8L6; [b]Dana-Farber Cancer Institute, Boston, MA 02115; [c]Institute for Systems Biology, Seattle, WA 98103; and [d]Department of Cellular and Molecular Medicine, University of Ottawa, Ottawa, ON, Canada K1H 8L6

Edited by Mark T. Groudine, Fred Hutchinson Cancer Research Center, Seattle, WA, and approved September 4, 2009 (received for review June 16, 2009)

Using a proteomics screen, we have identified the methyltransferase G9a as an interacting partner of the hematopoietic activator NF-E2. We show that G9a is recruited to the β-globin locus in a NF-E2-dependent manner and spreads over the entire locus. While G9a is often regarded as a corepressor, knocking down this protein in differentiating adult erythroid cells leads to repression of the adult β^{maj} *globin* gene and aberrant reactivation of the embryonic *β-like globin* gene E^{γ}. While in adult cells G9a maintains E^{γ} in a repressed state via dimethylation of histone H3 at lysines 9 and 27, it activates β^{maj} transcription in a methyltransferase-independent manner. Interestingly, the demethylase UTX is recruited to the β^{maj} (but not the E^{γ}) promoter where it antagonizes G9a-dependent H3K27 dimethylation. Collectively, these results reveal a dual role for G9a in maintaining proper expression (both repression and activation) of the β-globin genes in differentiating adult erythroid cells.

chromatin | histone methylation | UTX | NF-E2

Histone post-translational modifications play an important role in regulating chromatin-based cellular processes, including gene expression (1). Indeed, a strong correlation exists between the expression status of a gene and specific histone modifications. For example, methylation of histone H3 at lysine 4 (H3K4me) is a mark of active genes (2, 3). In contrast, methylation of histone H3 at lysine 9 (H3K9me) has been correlated with gene repression (1–3). Accordingly, all functionally characterized H3K9 methyltransferases (MTs), including Suv39H1 (KMT1A), Suv39H2 (KMT1B), Eset/SetDB1 (KMT1E), Riz1 (KMT8), G9a (KMT1C), and GLP/EuHMTase (KMT1D), have been implicated in gene silencing (1, 4). While Suv39H1 and Suv39H2 act mostly to promote the formation of pericentric heterochromatin, G9a and its interacting partner GLP represent major euchromatic H3K9 MTs since knockout of either one of these closely related enzymes leads to decreased levels of H3K9me2 in the euchromatic compartment of the nucleus (5, 6). At the functional level, G9a is essential for embryonic development (5) and has been implicated in the repression of a number of genes (7). Despite this largely documented repressor function, two reports have suggested that G9a might be involved in the activation of nuclear receptor-regulated genes (8) and genes transcribed by RNA Pol I (9). However, the molecular basis for this intriguing dual role in gene expression has not been resolved.

Interestingly, chromatin immunoprecipitation (ChIP) studies have revealed complex transitions between active and repressive histone methylation marks on a number of tissue-specific genes, suggesting that histone methylation might play an important, yet complex role in regulating cell differentiation (2). This complexity is particularly evident at the active β^{maj} *globin* gene, which is targeted by both H3K4 and H3K9 methylation in erythroid cells (10–12). We have recently shown that the transcription factor NF-E2 is involved in mediating H3K4 trimethylation (H3K4me3) at the β^{maj} *globin* gene via recruitment of the trithorax MT complex ASH2L/MLL2 (12). However, it is not clear how the H3K9 methyl mark is established at the active β^{maj} *globin* gene during terminal erythroid differentiation.

Results

The Hematopoietic Activator NF-E2/p45 Interacts with G9a in Erythroid Cells. Insight into how the H3K9 methyl marks are established on the β-globin locus came from the identification of the H3K9 MT G9a in a proteomics screen for NF-E2/p45-interacting proteins during erythropoiesis. Indeed, we identified both G9a and its dimerization partner GLP with a ProteinProphet score (13) of 99 and 100%, respectively. To confirm the interaction of G9a and GLP with NF-E2/p45 in nuclear extracts prepared from differentiated erythroid cells, we performed reciprocal immunoprecipitations (IP) using antibodies (Abs) recognizing the endogenous NF-E2/p45, GLP and G9a proteins (Fig. 1*A*). Western blot identified G9a and GLP [but not EZH2 (KMT6) or Pr-SET7/8 (KMT5A)] in the NF-E2/p45 IP while NF-E2/p45 was present in both G9a and GLP IPs. These results confirm the association of NF-E2/p45 with the G9a/GLP complex. To test whether NF-E2/p45 and G9a could directly interact, recombinant (rec) NF-E2/p45 and G9a proteins were incubated before IP with anti-G9a Abs. As shown on Fig. 1*B*, rec-NF-E2/p45 (but not rec-UBC4 protein) was precipitated by G9a Abs only in the presence of rec-G9a. This shows that NF-E2/p45 can interact directly with G9a.

We have shown previously that NF-E2/p45 associates with the MLL2-containing H3K4 MT complex (12). To determine whether NF-E2/p45-associated proteins also modify H3K9, we performed a MT assay using purified histone H3 as a substrate. Edman degradation revealed that H3K9 (and not H3K4) is the main target for methylation by NF-E2-associated proteins in this assay, confirming the association of NF-E2/p45 with an active H3K9 MT (Fig. 1*C*, left). Furthermore, it suggests that the activity of the G9a/GLP complex is dominant over that of the MLL2 complex in the assayed conditions. We reasoned that since H3K4 and H3K9 methylation inhibits each other in vitro (14), it is possible that G9a-induced methylation of H3K9 inhibits methylation of H3K4 in our assay. Since histone acety-

Author contributions: C.-P.C., A.M.H., F.J.D., and M.B. designed research; C.-P.C., A.M.H., C.P., J.A.R., and M.B. performed research; Y.N. and F.J.D. contributed new reagents/analytic tools; C.-P.C., A.M.H., C.P.-I., J.A.R., and M.B. analyzed data; and M.B. wrote the paper.

The authors declare no conflict of interest.

This article is a PNAS Direct Submission.

Data deposition: The data reported in this paper have been deposited in the Gene Expression Omnibus (GEO) database, www.ncbi.nlm.nih.gov/geo (accession no. GSE15620).

[1]C.-P.C. and A.M.H. contributed equally to this work.

[2]To whom correspondence should be addressed. E-mail: mbrand@ohri.ca.

This article contains supporting information online at www.pnas.org/cgi/content/full/0906769106/DCSupplemental.

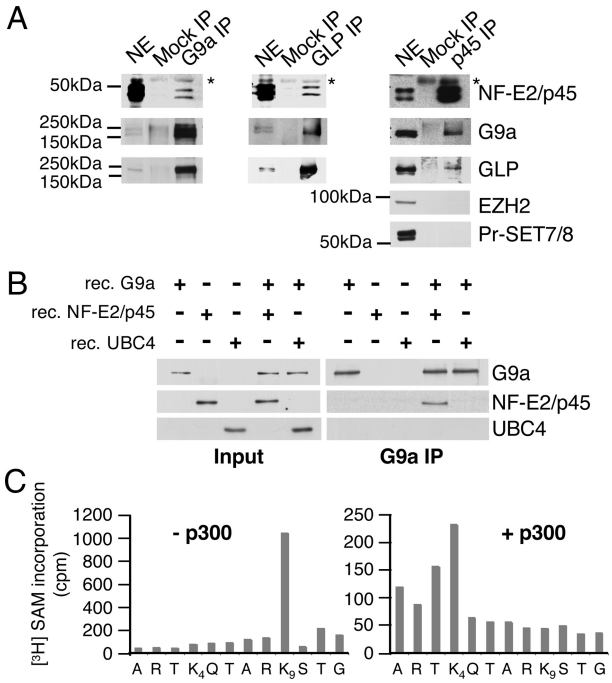

Fig. 1. NF-E2/p45 interacts with the H3K9 MT complex G9a/GLP. (*A*) Western blot analysis of endogenous proteins immunoprecipitated from an erythroid nuclear extract via Abs against NF-E2/p45, GLP and G9a. Abs used for Western blot are indicated on the right. Asterisk indicates Ab heavy chain. (*B*) Recombinant UBC4 or NF-E2/p45 proteins were incubated with recombinant G9a protein before G9a IP. (*C*) Histone H3 previously acetylated with p300 (+p300) or not (-p300) was used as a substrate for methylation by NF-E2/p45-interacting proteins and submitted to Edman degradation sequencing. The incorporated [^{3}H]-methyl at each amino acid is indicated in cpm.

lation correlates with H3K4me3 genome-wide (15), we used acetylated histone H3 as a methylation substrate (Fig. 1*C*, right). We found that under those conditions, the site of methylation by NF-E2-associated proteins switches from K9 to K4. While NF-E2/p45 interacts with both G9a and MLL2, these complexes do not directly associate (Fig. S1). These experiments, together with our previously published data (12), reveal that NF-E2/p45 interacts with two distinct and competing histone H3 MTs: the G9a/GLP complex, which methylates H3K9, and the MLL2 complex, which methylates H3K4.

Knockdown of G9a in Erythroid Cells Leads to Reduced Levels of both H3K9me2 and H3K27me2 Marks. To examine the role of G9a in erythropoiesis, we used RNA interference to knockdown (KD) this protein in differentiating adult erythroid cells. Two clonal mouse erythroleukemia (MEL) cell lines expressing doxycyclin (Dox)-inducible small hairpin (sh)RNA sequences were generated against different regions of the G9a coding sequence. In both clone 1 and clone 2, Dox treatment leads to a significant decrease of G9a (Fig. 2*A*). Next, we examined the effect of G9a KD on bulk histones by Western blot. Consistent with previous studies (5), loss of G9a leads to a significant decrease of H3K9me2 (Fig. 2 *B* and *C*). Interestingly, even though the H3K27 MT EZH2 (16) remains constant upon G9a KD (Fig. 2*A*), a decrease in the overall level of the repressive H3K27me2 mark was detected following G9a KD. This suggests that G9a can methylate H3K9 and K27 in erythroid cells.

Knocking Down G9a in Differentiating Erythroid Cells Leads to Reactivation of the Embryonic *E^y-Globin* and Downregulation of the Adult *β^{maj}* and *β^{min} Globin* Genes. While G9a KD did not affect MEL cell proliferation, we observed a significant decrease in hemoglobinization after induction of differentiation (Fig. S2). To test whether this defect is due to a deregulation of *β-globin* transcription, we used reverse transcription real-time quantitative PCR (RT-qPCR) to measure the different *β-globin* transcripts (Fig. 2 *D* and *E* and Fig. S3). We found that reduced levels of G9a during erythroid differentiation lead to a dose-dependent decrease (50–80%) of the adult β^{maj} and β^{min} *globin* transcripts. In contrast, the embryonic E^y *globin* gene is aberrantly upregulated upon G9a KD in both clones (Fig. 2*E* and Fig. S3). This effect is specific to G9a since KD of the repressive EZH2 (16) and EZH1 (17, 18) H3K27 MTs during erythroid differentiation does not lead to reactivation of E^y (Fig. S4). Furthermore, transcription of the other embryonic *β-globin* gene (β^{H1}), as well as genes from the heme biosynthesis pathway that are upregulated during DMSO-induced differentiation of MEL cells (i.e., PBGD and FECH), are not affected by G9a KD (Fig. 2 *D* and *E*). Finally, expression-profiling experiments on microarray in the G9a KD vs. wild-type (WT) differentiated MEL cells produced two very similar transcriptional profiles (Fig. S5). Notably, transcription factors important for erythroid differentiation such as GATA1, FOG1, NF-E2/p45, and EKLF are not modified upon G9a KD indicating that loss of G9a does not lead to an overall block of erythroid differentiation.

To verify whether changes in the levels of *β-globin* transcripts reflect alterations in RNA polymerase II (Pol II) binding, we used ChIP to examine the recruitment of this enzyme after G9a KD (Fig. 2*F*). While Pol II binding increases on the β^{maj} *globin* as it becomes expressed during differentiation, KD of G9a leads to a reduction in Pol II binding to both the promoter and coding region of this gene. In contrast, Pol II binding is increased on the E^y gene in parallel with reactivation of E^y transcription after G9a KD. Notably, the relative enrichment of Pol II at E^y vs. β^{maj} *globin* after G9a KD correlates with the relative levels of gene-specific transcription. Therefore, these ChIP results confirm the repression of β^{maj} and reactivation of E^y transcription upon G9a KD that were observed by RTqPCR. Collectively, our results suggest that G9a has a dual role in maintaining the embryonic E^y gene in a repressed state and activating the adult *β-globin* genes during differentiation of adult erythroid cells.

G9a Is Recruited to the *β-Globin* Locus in a NF-E2/p45-Dependent Manner and Directly Targets both the Embryonic and Adult *β-Globin* Genes. To determine whether G9a directly binds to the E^y and β^{maj} *globin* genes, we performed ChIP experiments across the β-globin locus under three conditions: nondifferentiated cells (Nondiff.), differentiated cells (Diff.) and cells differentiated in the presence of reduced levels of G9a (Diff. G9a KD) (Fig. 3*A*). Specificity for the G9a ChIP is demonstrated by the significant decrease of the ChIP signal after induction of G9a KD. First, we note that G9a is recruited to the HS2 site of the LCR during differentiation. Furthermore, G9a enrichment at this location coincides with that of the G9a-interacting erythroid protein NF-E2/p45, whose binding is not affected by G9a KD. Finally, G9a is recruited to the β-globin locus in a NF-E2/p45-dependent manner since G9a binding is lost in the NF-E2/p45-null murine erythroleukemia cell line CB3 (19) and restored in a CB3 clone stably expressing an exogenous NF-E2/p45 protein (Fig. S6). In contrast to NF-E2/p45, which localizes mainly at the LCR [Fig. 3*A* and (20)], G9a spreads within the β-globin locus after differentiation, targeting both the E^y and β^{maj} *globin* genes (Fig. 3*A* and Figs. S7 and S8). This result is reminiscent of the spreading of the MLL2 MT that we have previously described (12) and further suggests that G9a directly regulates E^y and β^{maj} *globin* transcription. Interestingly, the sites of G9a accumulation during erythroid differentiation differ between the embryonic and adult *β-globin* genes. Indeed, on the repressed E^y gene, the increase in G9a binding is the highest on the promoter region

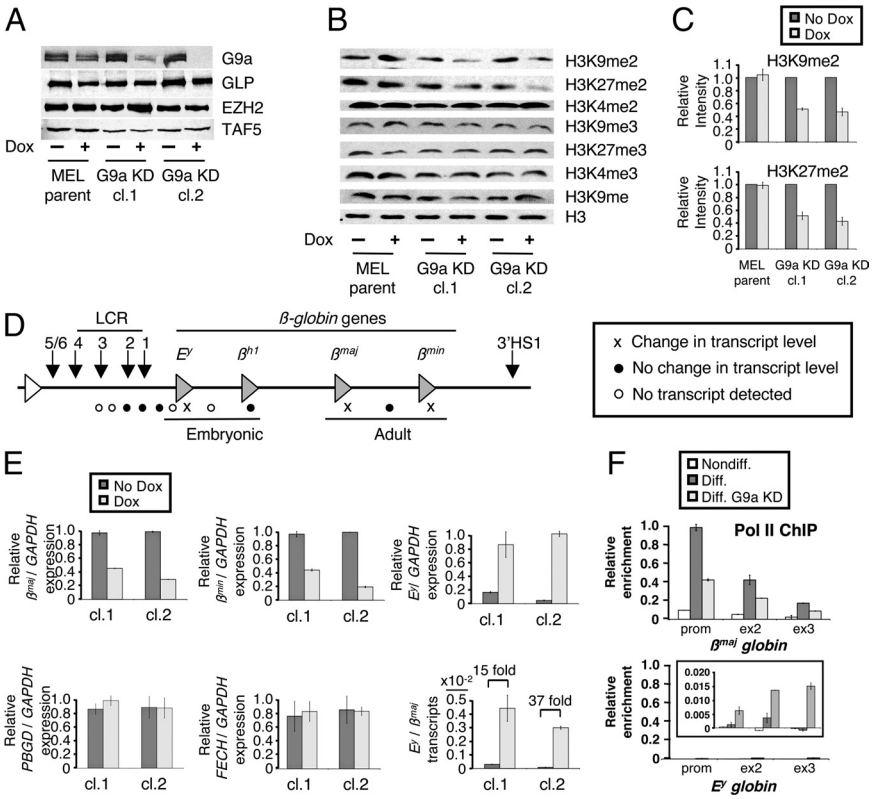

Fig. 2. G9a has a dual role in regulating expression of β-*globin* genes. (*A*) The expression of G9a and GLP was analyzed by Western blot after Dox-induced KD of G9a for two independent MEL clones (cl.1 and cl.2) targeting different regions of the G9a transcript. (*B*) Bulk cellular levels of H3K9me2, H3K27me2, and other histone modifications were analyzed by Western blot before and after G9a KD as indicated. (*C*) Relative enrichment of H3K9me2 and H3K27me2 as analyzed by Western blot in (*B*) are quantitated. Average ± SD represent three independent experiments. (*D*) Schematic representation of the murine β-globin locus. Shaded triangles represent the β-*like globin* genes. The white triangle represents the inactive olfactory receptor gene. Probes used to detect transcripts on the β-globin locus by RT-qPCR are labeled according to the variation of the transcripts levels upon G9a KD as indicated. (*E*) Transcription at the indicated genes was assessed by RT-qPCR after differentiation in G9a-depleted (Dox) vs. normal (No Dox) MEL cells. Transcripts are expressed relative to GAPDH with the highest ratio set to 1 or as a percentage of the E^y transcript relative to the β^{maj} transcript as indicated. Average values ± SD represent three independent experiments. (*F*) ChIPs were performed before (Nondiff.) and after induction of differentiation in G9a-depleted (Diff. G9a KD) vs. normal (Diff.) MEL cells to analyze the binding of the RPB1 subunit of Pol II. ChIPs were revealed by qPCR using TaqMan probes located within the promoter (prom), exon 2 (ex2), and exon 3 (ex3) of the globin genes as indicated. Values are expressed as a function of the highest enrichment and represent average of at least two replicates ± SD.

whereas on the active β^{maj} gene, G9a binding increases mostly within the coding region (Fig. 3*A*).

G9a Establishes H3K9 and H3K27 Dimethylation to Repress E^y Transcription. Since we observed a reduction in the bulk levels of H3K9me2 and H3K27me2 upon G9a KD (Fig. 2 *B* and *C*), we next examined the methylation status of these histone H3 residues on the β-*globin* locus. ChIP experiments revealed that H3K9me2 increases on the repressed E^y gene during differentiation, most strongly on the promoter region (Fig. 3*A*). In contrast, on the β^{maj} gene, which is activated during differentiation, the H3K9me2 mark increases on the coding region but remains constant on the promoter. These results are in agreement with previously published experiments that have correlated H3K9 methylation on promoters with gene repression while some active genes, including β^{maj} *globin* (11), exhibit H3K9 methylation in their coding regions (2, 3, 15). Importantly the pattern of H3K9me2 ChIP signal correlates with that of G9a on both E^y and β^{maj} *globin* genes (Fig. 3*A*) and decreases upon G9a KD. In contrast to H3K9me2, the G9a-dependent increase in H3K27me2 mark is limited to the repressed embryonic E^y *globin* gene (Fig. 3*A*). Importantly, methylation of H3K27 is a marker for repressed genes and often correlates with methylated H3K9 (15), suggesting that the combination of these two methylation marks maintain efficient repression of E^y.

To address more directly the involvement of G9a and its MT activity in the repression of E^y and the activation of β^{maj} *globin*, we attempted to rescue the G9a KD by ectopic expression of shRNA-resistant wild-type (WT) G9a or a MT-defective mutant (5). We found that the WT G9a protein was able to restore repression of the embryonic E^y gene while the MT-defective mutant was unable to do so (Fig. 3*B*). This result confirms that the MT activity of G9a is required for its repressive function on the E^y *globin* gene. Furthermore, ChIP experiments show that WT G9a, but not the MT-defective mutant, rescues both the H3K9me2 and the H3K27me2 marks on the E^y promoter (Fig. 3*B*). This strongly suggests that G9a maintains the embryonic E^y *globin* gene in a transcriptionally repressed state via dimethylation of both H3K9 and H3K27. In contrast, the activating function of G9a toward the adult β^{maj} *globin* gene appears independent of its MT activity. Indeed both WT G9a and the MT-defective mutant are able to restore full β^{maj} *globin* transcription in G9a KD cells (Fig. 3*B*). To get further insight into the molecular mechanism by which G9a stimulates transcription of the adult β^{maj} *globin* gene, we examined the effect of G9a KD on histone marks that have been correlated with active genes (e.g., H3K4me3 and H3K36me3). ChIP experiments show that the decrease of β^{maj} transcription after G9a KD is associated with a significant reduction of H3K36me3 whereas the H3K4me3 mark persists on this gene (Fig. S9*B*). In agreement

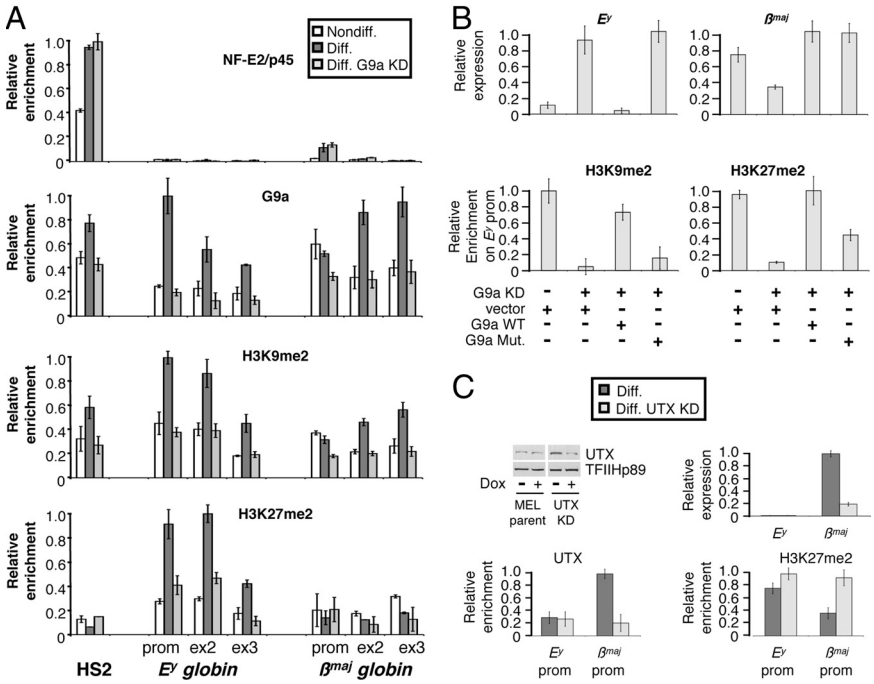

Fig. 3. G9a-dependent histone methylation on the β-globin locus. (*A*) ChIPs were performed before (Nondiff.) and after differentiation in G9a-depleted (Diff. G9a KD) vs. normal (Diff.) MEL cells to analyze the binding of NF-E2/p45 and G9a as well as the enrichment of H3K9me2 and H3K27me2. ChIPs were revealed by qPCR using indicated probes. Values are expressed as a function of the highest enrichment and represent average of at least two replicates ± SD. (*B*) RT-qPCR analysis of the embryonic E^y and adult β^{maj} *globin* genes was performed upon differentiation in G9a KD cells after transfection of DNA constructs expressing WT G9a (WT) or a MT-defective G9a mutant (Mut.). These constructs were rendered resistant to shRNA-mediated KD of G9a via silent mutations (sequences available in *SI Text*). Transcripts values are expressed relative to GAPDH with the highest ratio set to 1. Average values ± SD represent three independent experiments. ChIPs were performed in the same conditions to analyze the enrichment of the H3K9me2 and H3K27me2 on the E^y *globin* promoter. ChIPs were revealed by qPCR. Values are expressed as a function of the highest enrichment and represent average of at least two replicates ± SD. (*C*) UTX and TFIIHp89 proteins levels were analyzed by Western blot after Dox-induced KD of UTX in differentiating MEL cells. Transcription at the E^y and β^{maj}-*globin* genes was assessed by RT-qPCR after differentiation in UTX-depleted (Diff.UTX KD) vs. normal (Diff.) MEL cells. Transcripts values are expressed relative to GAPDH with the highest ratio set to 1. ChIPs were performed after differentiation in UTX-depleted vs. normal MEL cells to analyze the binding of UTX and the enrichment of H3K27me2. ChIPs were revealed by qPCR using probes located at the promoters of the E^y and β^{maj} *globin* genes. Values are expressed as a function of the highest enrichment and represent average of at least two replicates ± SD.

with the fact that the H3K4me3 mark, which stabilizes $TF_{II}D$ on gene promoters (21), is still present after G9a KD, we did not detect a significant change in $TF_{II}D$ binding on the β^{maj} promoter following G9a KD (Fig. S9*C*). In contrast, G9a KD profoundly affects Pol II, $TF_{II}F$, $TF_{II}H$, and Mediator recruitment to the β^{maj} gene (Fig. 2*F* and Fig. S9*C*). Finally, we found that G9a interacts with Pol II (Fig. S9*A*). Collectively, these results suggest that G9a is involved in stabilizing PIC formation independently of $TF_{II}D$ binding.

While the transactivation function of G9a does not require histone methylation (Fig. 3*B*) and (8), the question remains as to why the MT-bound β^{maj} *globin* gene does not become enriched for the repressive H3K27me2 mark. A possibility is that the H3K27me2 mark could be actively removed from the adult β^{maj} *globin* gene via a demethylase. We found that the H3K27 demethylase UTX (22) is recruited to the β^{maj} but not the E^y promoter during differentiation. In addition, KD of UTX in differentiated MEL cells leads to a decrease in β^{maj} *globin* transcription with a concurrent increase of the H3K27me2 mark at the gene promoter (Fig. 3*C*). This active removal of the H3K27me2 mark from the adult β^{maj} globin gene provides a mechanism by which UTX antagonizes the repressive G9a-dependent H3K27me2 mark, permitting this dual-function protein to activate transcription of the β^{maj} *globin* gene.

Discussion

By knocking down G9a, we have shown that this protein is involved in maintaining proper expression of the β-*globin* genes in differentiating adult erythroid cells. While G9a is often regarded as a corepressor, we found that reducing the level of G9a during adult erythroid differentiation leads to aberrant activation of the embryonic β-*like globin* gene E^y and the concurrent repression of its adult homologs β^{maj} and β^{min}. Moreover, we provide evidence that G9a is directly involved in mediating these opposite transcriptional activities on the β-globin locus.

The Repressive Role of G9a. G9a has been shown to methylate both H3K9 and H3K27 in vitro (23, 24). It has been questioned whether G9a methylates H3K27 in vivo (5). However, another study showed that H3K9me2 and H3K27me2 marks are reduced at multiple loci in $G9a^{-/-}$ ES cells (25). In agreement with this last study, we show that reducing the level of G9a in erythroid cells leads to a significant decrease in bulk- and E^y gene specific-levels of H3K9me2 and H3K27me2. Supporting a role for G9a in mediating H3K27 dimethylation on the β-globin locus, the KD of EZH2 and EZH1 in differentiating erythroid cells does not lead to reactivation of E^y transcription. Finally, expression of an exogenous wild-type G9a protein (but not a MT mutant) in G9a KD cells is sufficient to rescue both H3K9me2 and H3K27me2 marks on the E^y gene promoter. Together these results strongly suggest that G9a is responsible for dimethylating both H3K9 and H3K27 on the E^y gene. However we cannot completely exclude the possibility that G9a-dependent H3K9me2 mark might recruit EZH1/2 MTs, which would mediate H3K27 dimethylation at the E^y *globin* gene.

The Activating Role of G9a. G9a activation of the β^{maj} *globin* gene was shown to be independent of G9a MT activity. This is in agreement with a previous study showing that the MT activity of G9a is not required for its role as a coactivator of nuclear receptor-dependent genes (8). Examining the different steps of transcriptional initiation, we were able to identify a function for G9a in establishing a competent PIC at the β^{maj} promoter. Our ChIP data show that with the noticeable exception of $TF_{II}D$, G9a KD in differentiating erythroid cells leads to significant defects in the binding of the general transcription factors on the β^{maj} promoter (Fig. 2*F* and Fig. S9*C*). Together with the interaction between G9a and Pol II (Fig. S9*A*), this result supports a role for G9a in facilitating PIC formation on the promoter independently of $TF_{II}D$ binding. It remains to be determined whether this role in PIC formation is mediated through G9a's ability to cooperate with the coactivators GRIP1, CARM1, and p300 (8).

What Dictates Whether G9a Is Going to Be an Activator or a Repressor? The most striking result from our study is that G9a displays opposite roles on homologous genes, which are located within the same locus, yet are normally expressed at different developmental stages. We have shown that methylation of both H3K9 and H3K27 on the gene promoter are implicated in G9a repressive function, whereas G9a activating role involves facilitating PIC formation on the active gene promoter. Several mechanisms may be important in modulating G9a function. First, previously established histone modifications might affect G9a MT activity. For example, acetylation of histone H3 (this study) and methylation of H3K4 (14) both inhibit H3K9 methylation in vitro. Interestingly, it has been shown previously that in adult erythroid cells, the β^{maj} gene is enriched in acetylated histone H3, H3K4me2, and H3K4me3, while these marks are considerably reduced on the E^{y} gene (10, 12). Second, histone marks that are established by G9a might be removed by competing enzymes, ultimately modifying the transcriptional status of the target gene. Indeed the H3K27 demethylase UTX (22) is selectively enriched on the β^{maj} *globin* promoter (but not the E^{y} promoter) in differentiated erythroid cells. In addition, KD of UTX in these cells leads to a decrease of β^{maj} *globin* transcription and a concurrent increase of the H3K27me2 mark on this gene. Collectively, these results suggest that UTX may be involved in counteracting the repressive function of G9a via active removal of the H3K27me2 mark from the β^{maj} *globin* promoter in differentiated cells. In conclusion, the decision of whether G9a will act as a repressor or activator involves complex regulatory mechanisms that are highly context-dependent and might have been established earlier in development.

Implications of G9a Function in Maintaining the Expression Program on the β-globin Locus. The *β-globin* genes are organized in a cluster and are transcribed at specific stages during development. What establishes and maintains this developmentally regulated expression program is unclear. The prevalent model is that the *β-globin* genes compete for binding to the distal LCR, with the gene closest to the LCR being activated in priority unless silenced autonomously (26). However, on the murine β-globin locus, the genes are not organized in their developmental order of expression (27). Also, even though the LCR promotes an extremely high-level of β-globin transcription [by forming a local environment enriched in transcription factors within a "Pol II factory" (28) and/or "chromatin hub" (29)], deletion of the murine LCR did not perturb the developmental timing of expression of β-globin genes (30). Our findings provide evidence that maintenance of the expression program of *β-globin* genes in adult red cells is regulated via epigenetic mechanisms, with an important role played by G9a. Furthermore, we show that this process does not involve competition between the embryonic E^{y} and the adult β^{maj} *globin* for binding to the LCR since both genes can be activated simultaneously in the presence of a MT-defective G9a mutant.

Interestingly, two epigenetic factors, MLL2 (12) and G9a (this study), display a common mode of binding to chromatin. Following recruitment via the NF-E2/p45 activator, which localizes to defined sites, both enzymes cover the entire β-globin locus. Therefore, while looping of the LCR might be important for transferring general transcription factors to the distal *β-globin* genes (29), our results suggest that histone MTs preferentially follow a previously proposed linking mechanism (31) whereby they spread the length of the locus. Importantly, while MLL2 and G9a can be found across the β-globin locus, their respective MT activities appear to be modulated through additional mechanisms.

We have shown that G9a is important for maintaining the proper gene expression program at the β-globin locus in erythroid cells and have identified molecular determinants of G9a's opposite role in repressing embryonic and activating adult *β-like globin* genes. Additional studies aimed at understanding the interdependence of epigenetics factors on the β-globin locus should provide further insights into the spatio-temporal regulation of β-globin transcription.

Materials and Methods

Cell Culture, Erythroid Differentiation, Nuclear Extraction, Immunoprecipitation, and Mass Spectrometry. These procedures were performed as described in (12, 32) using MEL cells (clone 745) which are blocked at the pro-erythroblast stage and serve as a model system for terminal erythroid differentiation in the definitive lineage. In these cells, treatment with DMSO induces erythroid differentiation including activation of the adult *β-globin* genes and hemoglobin synthesis (20, 33). The murine erythroleukemia CB3 cell line that does not express NF-E2/p45 was previously described (19).

MT Assays. The assay was performed as described in (12) with modifications in *SI Text*.

G9a, EZH2, and UTX Knockdown in MEL Cells. Stable MEL cell lines, expressing a Dox-dependent shRNA sequence targeting G9a, EZH2, or UTX mRNA were established as previously described (12). The KD was induced by 5 μg/mL Dox. Sequences available in *SI Text*.

G9a KD Rescue. G9a expression constructs used for rescuing the G9a KD were a kind gift from Y. Shinkai (Kyoto University, Japan) and have been described previously (5). Using the QuikChange XL site-directed mutagenesis kit (Stratagene), silent mutations (*SI Text*) were introduced into the G9a sequence such that the exogenous G9a transcript expressed from these constructs is resistant to anti-G9a shRNA. These modified G9a constructs were electroporated into the G9a KD inducible MEL cells (clone 2) 6 h before Dox induction, and the RNA (for RT-qPCR) and chromatin (for ChIP) were extracted after 4 days of DMSO-induced differentiation.

Expression Profiling on Affymetrix Microarray. Procedure described in *SI Text*.

Chromatin Immunoprecipitation. For ChIPs using anti-histone Abs, we used a native ChIP protocol (34, 35) and for all other ChIPs, we used a crosslink ChIP protocol as described in (12). A list of Abs is provided as *SI Text*. Fractions of input are calculated and subsequently normalized in function of the highest enrichment on the locus as previously described (12, 35).

ACKNOWLEDGMENTS. We thank A. Dean and M. Lorincz for critically reading the manuscript; P. Chambon, S. Pradhan, P. Rakopoulos (The Sprott Center for Stem Cell Research, Regenerative Medicine Program, Ottawa Hospital Research Institute, Ottawa, ON Canada), Y. Shinkai, and L. Tora for providing reagents; A. Desjardins for technical help; G. Palidwor for microarray data analysis; and F. Dumas for Edman sequencing. This project was funded with grants from the Canadian Institutes of Health Research and the Terry Fox Foundation (Canadian Cancer Society Research Institute) (to to M.B.) and a CIHR/Thalassemia Foundation of Canada fellowship (to C-P.C.). M.B. holds the Canadian Research Chair in the regulation of gene expression.

1. Li B, Carey M, Workman JL (2007) The role of chromatin during transcription. *Cell* 128:707–719.
2. Mikkelsen TS, et al. (2007) Genome-wide maps of chromatin state in pluripotent and lineage-committed cells. *Nature* 448:553–560.
3. Barski A, et al. (2007) High-resolution profiling of histone methylations in the human genome. *Cell* 129:823–837.
4. Shilatifard A (2008) Molecular implementation and physiological roles for histone H3 lysine 4 (H3K4) methylation. *Curr Opin Cell Biol* 20:341–348.
5. Tachibana M, et al. (2002) G9a histone methyltransferase plays a dominant role in euchromatic histone H3 lysine 9 methylation and is essential for early embryogenesis. *Genes Dev* 16:1779–1791.
6. Rice JC, et al. (2003) Histone methyltransferases direct different degrees of methylation to define distinct chromatin domains. *Mol Cell* 12:1591–1598.
7. Ogawa H, Ishiguro K, Gaubatz S, Livingston DM, Nakatani Y (2002) A complex with chromatin modifiers that occupies E2F- and Myc-responsive genes in G0 cells. *Science* 296:1132–1136.
8. Lee DY, Northrop JP, Kuo MH, Stallcup MR (2006) Histone H3 lysine 9 methyltransferase G9a is a transcriptional coactivator for nuclear receptors. *J Biol Chem* 281:8476–8485.
9. Yuan X, Feng W, Imhof A, Grummt I, Zhou Y (2007) Activation of RNA polymerase I transcription by cockayne syndrome group B protein and histone methyltransferase G9a. *Mol Cell* 27:585–595.
10. Bulger M, et al. (2003) A complex chromatin landscape revealed by patterns of nuclease sensitivity and histone modification within the mouse beta-globin locus. *Mol Cell Biol* 23:5234–5244.
11. Vakoc CR, Mandat SA, Olenchock BA, Blobel GA (2005) Histone H3 lysine 9 methylation and HP1gamma are associated with transcription elongation through mammalian chromatin. *Mol Cell* 19:381–391.
12. Demers C, et al. (2007) Activator-mediated recruitment of the MLL2 methyltransferase complex to the beta-globin locus. *Mol Cell* 27:573–584.
13. Nesvizhskii AI, Keller A, Kolker E, Aebersold R (2003) A statistical model for identifying proteins by tandem mass spectrometry. *Anal Chem* 75:4646–4658.
14. Wang H, et al. (2001) Purification and functional characterization of a histone H3-lysine 4-specific methyltransferase. *Mol Cell* 8:1207–1217.
15. Wang Z, et al. (2008) Combinatorial patterns of histone acetylations and methylations in the human genome. *Nat Genet* 40:897–903.
16. Cao R, Zhang Y (2004) The functions of E(Z)/EZH2-mediated methylation of lysine 27 in histone H3. *Curr Opin Genet Dev* 14:155–164.
17. Margueron R, et al. (2008) Ezh1 and Ezh2 maintain repressive chromatin through different mechanisms. *Mol Cell* 32:503–518.
18. Shen X, et al. (2008) EZH1 mediates methylation on histone H3 lysine 27 and complements EZH2 in maintaining stem cell identity and executing pluripotency. *Mol Cell* 32:491–502.
19. Lu SJ, Rowan S, Bani MR, Ben-David Y (1994) Retroviral integration within the Fli-2 locus results in inactivation of the erythroid transcription factor NF-E2 in Friend erythroleukemias: Evidence that NF-E2 is essential for globin expression. *Proc Natl Acad Sci USA* 91:8398–8402.
20. Sawado T, Igarashi K, Groudine M (2001) Activation of beta-major globin gene transcription is associated with recruitment of NF-E2 to the beta-globin LCR and gene promoter. *Proc Natl Acad Sci USA* 98:10226–10231.
21. Vermeulen M, et al. (2007) Selective anchoring of TFIID to nucleosomes by trimethylation of histone H3 lysine 4. *Cell* 131:58–69.
22. Agger K, Christensen J, Cloos PA, Helin K (2008) The emerging functions of histone demethylases. *Curr Opin Genet Dev* 18:159–168.
23. Tachibana M, Sugimoto K, Fukushima T, Shinkai Y (2001) Set domain-containing protein, G9a, is a novel lysine-preferring mammalian histone methyltransferase with hyperactivity and specific selectivity to lysines 9 and 27 of histone H3. *J Biol Chem* 276:25309–25317.
24. Rathert P, et al. (2008) Protein lysine methyltransferase G9a acts on non-histone targets. *Nat Chem Biol* 4:344–346.
25. Ikegami K, et al. (2007) Genome-wide and locus-specific DNA hypomethylation in G9a deficient mouse embryonic stem cells. *Genes Cells* 12:1–11.
26. Stamatoyannopoulos G (2005) Control of globin gene expression during development and erythroid differentiation. *Exp Hematol* 33:259–271.
27. Kingsley PD, et al. (2006) ''Maturational'' globin switching in primary primitive erythroid cells. *Blood* 107:1665–1672.
28. Ragoczy T, Bender MA, Telling A, Byron R, Groudine M (2006) The locus control region is required for association of the murine beta-globin locus with engaged transcription factories during erythroid maturation. *Genes Dev* 20:1447–1457.
29. Tolhuis B, Palstra RJ, Splinter E, Grosveld F, de Laat W (2002) Looping and interaction between hypersensitive sites in the active beta-globin locus. *Mol Cell* 10:1453–1465.
30. Bender MA, Bulger M, Close J, Groudine M (2000) Beta-globin gene switching and DNase I sensitivity of the endogenous beta-globin locus in mice do not require the locus control region. *Mol Cell* 5:387–393.
31. Bulger M, Groudine M (1999) Looping versus linking: Toward a model for long-distance gene activation. *Genes Dev* 13:2465–2477.
32. Ranish JA, Brand M, Aebersold R (2007) in *Quantitative Proteomics by Mass Spectrometry* (Humana Press, Clifton, NJ), pp 1064–3745.
33. Friend C, Scher W, Holland JG, Sato T (1971) Hemoglobin synthesis in murine virus-induced leukemic cells in vitro: Stimulation of erythroid differentiation by dimethyl sulfoxide. *Proc Natl Acad Sci USA* 68:378–382.
34. Rampalli S, et al. (2007) p38 MAPK signaling regulates recruitment of Ash2L-containing methyltransferase complexes to specific genes during differentiation. *Nat Struct Mol Biol* 14:1150–1156.
35. Brand M, Rampalli S, Chaturvedi CP, Dilworth FJ (2008) Analysis of epigenetic modifications of chromatin at specific gene loci by native chromatin immunoprecipitation of nucleosomes isolated using hydroxyapatite chromatography. *Nat Protoc* 3:398–409.

Supporting Information

Chaturvedi et al. 10.1073/pnas.0906769106

SI Text

Antibodies Used for Western Blot. From Santa Cruz Biotechnology, we used anti-$TF_{II}H$, XPB subunit (sc-293) and anti-NF-E2/p45 (sc-291). We also used the NF-E2/p45 Ab (#945) and ASH2L Ab (#1025) (1). From Perseus Proteomics, we used anti -G9a (PP-A8620A-00) and -GLP (PP-B0422–00). From Invitrogen, we used anti-EZH2 (36–6300). We also used the ActiveMotif anti-EZH2 (39103). The TAF5 Ab (2) was a gift from L. Tora (IGBMC, Strasbourg, France). From Abcam, we used anti -Pr-SET7/8 (ab3798), -H3K9me (ab9045), -H3K9me2 (ab1220), -H3K9me3 (ab8898), -H3K27me2 (ab24684), -H3K27me3 (ab6002), -H3K4me3 (ab8580), and unmodified H3 (ab10158). From Upstate/Millipore, we used anti-His tag (05–531) to detect UBC4, anti-H3K4me2 (07–030) and H3K27me2 (07–452). From Covance, we used Abs against non-phosphorylated Pol II (8WG16). From Bethyl, we used anti-MLL2 (BL-835).

Abs used for IP and ChIP are the same except that for the G9a ChIP, we used the Ab prepared in the Nakatani lab (3) and for the Pol II ChIP, we used a mixture of sc-5943, sc-17798, and sc-9001. For H3K27me2 ChIPs, in addition to the Abcam Ab, we also used the anti-H3K27me2 Ab from Diagenode (pAb-046–050), and obtained the same results with both Abs. Other ChIP Abs are: normal rabbit IgG (sc-2027), normal mouse IgG (sc-2025), anti-$TF_{II}F$ RAP74 subunit (sc-235), and H3K36me3 (ab9050). For the $TF_{II}D$ ChIP, we used a mixture of the 3G3 (4) and 2C1 (5) Abs against the TBP subunit (both gifts from L. Tora, IGBMC, Strasbourg, France). For the Mediator ChIP, we used Abs against the Med17 subunit (a gift from P. Chambon, IGBMC, Strasbourg, France). The UTX Ab has been generated in a rabbit using an antigen identical to that previously described (6).

Silent Mutations Introduced into the G9a Coding Sequence

G9a shRNA (clone 2)
GG GTG AAG CCA TCT AGA AA (original DNA sequence)
GG GTT AAA CCT AGC AGG AA (mutated DNA sequence)
V K P S R (protein sequence)

TaqMan Probes and Primers Used in Real-Time Quantitative PCR and RT-qPCR.

HS2
Forward primer CAGAGGAGGTTAGCTGGGCC
Reverse primer CAAGGCTGAACACACCCACA
TaqMan probe FAM- AGGCGGAGTCAATTCTCTACTC-CCCACC −BHQ_1
E^{y}prom
Forward primer CTTCAAAGAATAATGCAGAACA-AAGG
Reverse primer CAGGAGTGTCAGAAGCAAGTACGT
TaqMan probe FAM- ATTGTCTGCGAAGAATAAAAG-GCCACCACTT −BHQ_1
E^{y}ex2
Forward primer GCAAGAAGGTGCTGACTGCTT
Reverse primer GTAGCTTGTCACAGTGCAGTTCACT
TaqMan probe FAM- TGGAGAGTCCATTAAGAACCTA-GACAACCTCAAGTC–MGBNFQ
E^{y}ex3
Forward primer GCTAGTCACTTCGGCAATGAATT
Reverse primer CCCAGCCACCAGCTTCTG
TaqMan probe FAM TGAGATGCAGGCTGC-MGBNFQ
β^{maj} prom
Forward primer CTGCTCACACAGGATAGAGAGGG
Reverse primer GCAAATGTGAGGAGCAACTGATC
TaqMan probe FAM- AGCCAGGGCAGAGCATATAAG-GTGAGGT −BHQ_1
β^{maj} ex2
Forward primer GAAGGCCCATGGCAAGAAG
Reverse primer GCCCTTGAGGCTGTCCAA
TaqMan probe FAM- TGATAACTGCCTTTAACGATG-GCCTGAATCA −MGBNFQ
β^{maj} ex3
Forward primer TCTACAGTTATGTTGATGGTTCT-TCCA
Reverse primer CAGGACAATCACGATCATATTGC
TaqMan probe FAM- TCCCACAGCTCCTG −MGBNFQ
β^{min} ex3
Forward primer GCAATGCGATCGTGATTGTG
Reverse primer CAGCCACCACCTTCTGGAA
TaqMan probe FAM- CCCCTGCTGCACAGG−MGBNFQ
G9a
Forward primer AAAACCATGTCCAAACCTAGCAA
Reverse primer GCGGAAATGCTGGACTTCAG
TaqMan probe FAM- ACAGCCTCCAATCCCTGAGAA-GCGG −BHQ1
GLP
Forward primer TGTGTGACATCCCCCATGAA
Reverse primer GCAGTCATCTACACACACGCAGTA
TaqMan probe FAM- CAGGAACATCACTCATT−BHQ1
PBGD
Forward primer CGCATACAGACCGACACT
Reverse primer CAGGCTCTTCTCTCCAATCT
TaqMan probe FAM- TTGAAATCATTGCTATGTCCAC-CACGG −BHQ1
FECH
Forward primer CCCTTGGAGAAGTTCAAGAC
Reverse primer CGATTCTGCGATACTGCTCT
TaqMan probe FAM- CACTTCCCATTCAAAATAAGCT-GGCACC −BHQ1
EZH2
Forward primer TCAAAACCGCTTTCCTGG
Reverse primer TGTCCCAATGGTCAGCA
TaqMan probe FAM- AGTGTCCATGCTACCTGGCTGT −BHQ1
EZH1
Forward primer TTCCACGGCACCTATTTCAAC
Reverse primer TGTCTTTGTCCCCAGAAGCC
TaqMan probe FAM- ACTTCTGCTCAATAGCCA −BHQ1
FAM is the fluorophore.
BHQ, Black hole quencher
MGB, Minor groove binder
NFQ, Non fluorescent quencher
For GAPDH RT-qPCR, we used the rodent primers and probes kit from Applied Biosystems (Part no. 4308313).

shRNA Sequences Targeting G9a mRNA. 5′CCCTGATCTTT-GAGTGTAA3′ (clone 1)
5′GGGTGAAGCCATCTAGAAA3′ (clone 2)

shRNA Sequence Targeting EZH2 mRNA. 5′GGGAGAGAACAAT-GATAAA3′

shRNA Sequence Targeting UTX mRNA. 5′GCCAAAGGACAAGT-TGAAT3′

siRNA Sequences Targeting EZH1 mRNA. EZH1#1: 5′GAGGGAAGGUCUAUGAUAATT3′

EZH1#2: 5′UUUGCAAGACACCACCUUACAGUCC3′ (sequence from (7))

Luciferase Targeting Control siRNA. 5′AUCACAGAAUCGUCGUAUGTT3′

NF-E2p45/G9a Direct Interaction. Equivalent amounts of recombinant purified UBC4, NF-E2/p45, and G9a (8) (a kind gift from S. Pradhan, New England Biolabs) proteins were incubated on ice for 1 h in a buffer containing 100 mM KCl, 25 mM Tris, pH 7.9, 5 mM $MgCl_2$, 10% (vol/vol) glycerol, 0.1% (vol/vol) Nonidet P-40 substitute, 0.3 mM DTT, and protease inhibitors mixture, before immunoprecipitation with G9a Ab-coupled M280 Dynabeads (Invitrogen) for 2 h at 22 °C with constant shaking at 1,400 rpm. After extensive washing with the same buffer, bound proteins were eluted by boiling for 5 min with SDS-containing loading dye and analyzed by Western blot.

Real-Time RTqPCR Analysis. Total RNA was isolated using the RNeasy Mini Kit (Qiagen) according to the manufacturer's instructions, including the on-column DNase I digestion step. One-step real-time RTqPCR was done on a Rotorgene instrument 6000 (Corbett Research) using minor groove binder TaqMan probes (ABI) and primers.

Expression Profiling on Affymetrix Microarray. Total RNA (10 μg) was extracted and purified as described above from three independent biological replicates of the WT and corresponding G9a KD cells (six samples total). The quality of RNA was verified before labeling and hybridization to the Affymetrix Mouse Genome 430 2.0 gene expression microarray. Labeling and hybridization were performed at the Genome Sciences Center (BC Cancer Agency, British Columbia, Canada) following standard Affymetrix procedures. Intensity values were normalized using GC RMA (9).

Methyltransferase Assays. The assay was performed as described in (1) except that 1 mg/mL purified histone H3 (Roche) was used as a methylation substrate. After SDS/PAGE, transfer onto PVDF membrane and Coomassie staining, histone H3 was sequenced at the Biotechnology Research Institute (NRC, Montreal, QC, Canada) and the radioactivity was counted at each Edman degradation cycle. For the experiment where acetylated H3 is used as a methylation substrate, NF-E2/p45 associated proteins on beads were first incubated with 100 μg recombinant p300 in the presence of 12 μM acetyl-coA and 1 mg histone H3 for 45 min at 30 °C. Methylation was then initiated through adding 6.5 μM [^{3}H] s-adenosyl methionine.

1. Demers C, et al. (2007) Activator-mediated recruitment of the MLL2 methyltransferase complex to the beta-globin locus. *Mol Cell* 27:573–584.
2. Dubrovskaya V, et al. (1996) Distinct domains of hTAFII100 are required for functional interaction with transcription factor TFIIFbeta (RAP30) and incorporation into the TFIID complex. *EMBO J* 15:3693–3701.
3. Shi Y, et al. (2003) Coordinated histone modifications mediated by a CtBP co-repressor complex. *Nature* 422:735–738.
4. Brou C, et al. (1993) Distinct TFIID complexes mediate the effect of different transcriptional activators. *EMBO J* 12:489–499.
5. Jacq X, et al. (1994) Human TAFII30 is present in a distinct TFIID complex and is required for transcriptional activation by the estrogen receptor. *Cell* 79:107–117.
6. Issaeva I, et al. (2007) Knockdown of ALR (MLL2) reveals ALR target genes and leads to alterations in cell adhesion and growth. *Mol Cell Biol* 27:1889–1903.
7. Margueron R, et al. (2008) Ezh1 and Ezh2 maintain repressive chromatin through different mechanisms. *Mol Cell* 32:503–518.
8. Patnaik D, et al. (2004) Substrate specificity and kinetic mechanism of mammalian G9a histone H3 methyltransferase. *J Biol Chem* 279:53248–53258.
9. Wu Z, Irizarry RA, Gentleman R, Martinez-Murillo F, Spencer F (2004) A Model-Based Background Adjustment for oligonucleotide Expression Arrays. *J Am Stat Assoc* 99:909–917.

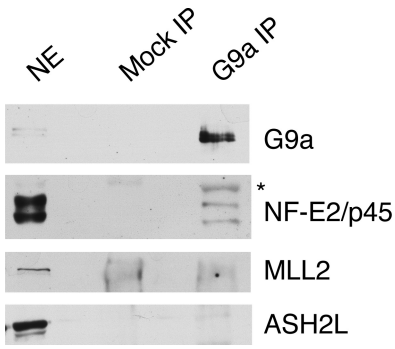

Fig. S1. G9a does not interact with the MLL2 complex in nuclear extracts from erythroid cells. Western blot analysis of endogenous proteins immunoprecipitated from an erythroid nuclear extract via Ab against G9a. Mock IP with normal mouse IgG was used as a negative control. Abs used for Western blot are indicated on the right. Asterisk indicates Ab heavy chain.

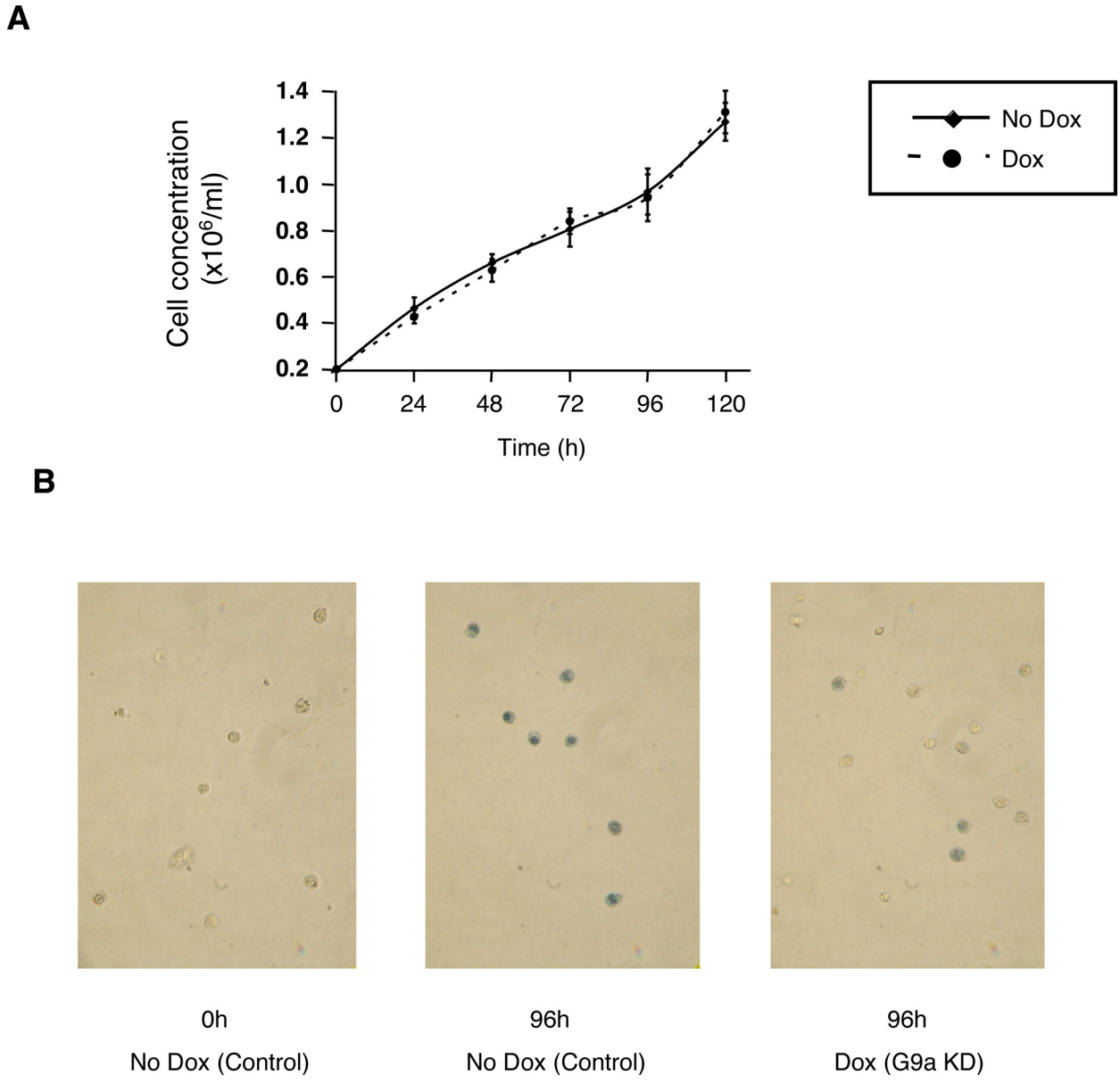

Fig. S2. G9a knockdown decreases hemoglobinization of erythroid cells without affecting cell growth. (*A*) Cell concentration was assessed every 24 h as indicated after induction of erythroid differentiation (0 h) in G9a-depleted (Dox) vs. normal (No Dox) MEL cells. (*B*) Hemoglobin content was assessed by benzidine staining in G9a depleted (Dox) vs. normal (No Dox) MEL cells before (0 h) and after (96 h) erythroid differentiation.

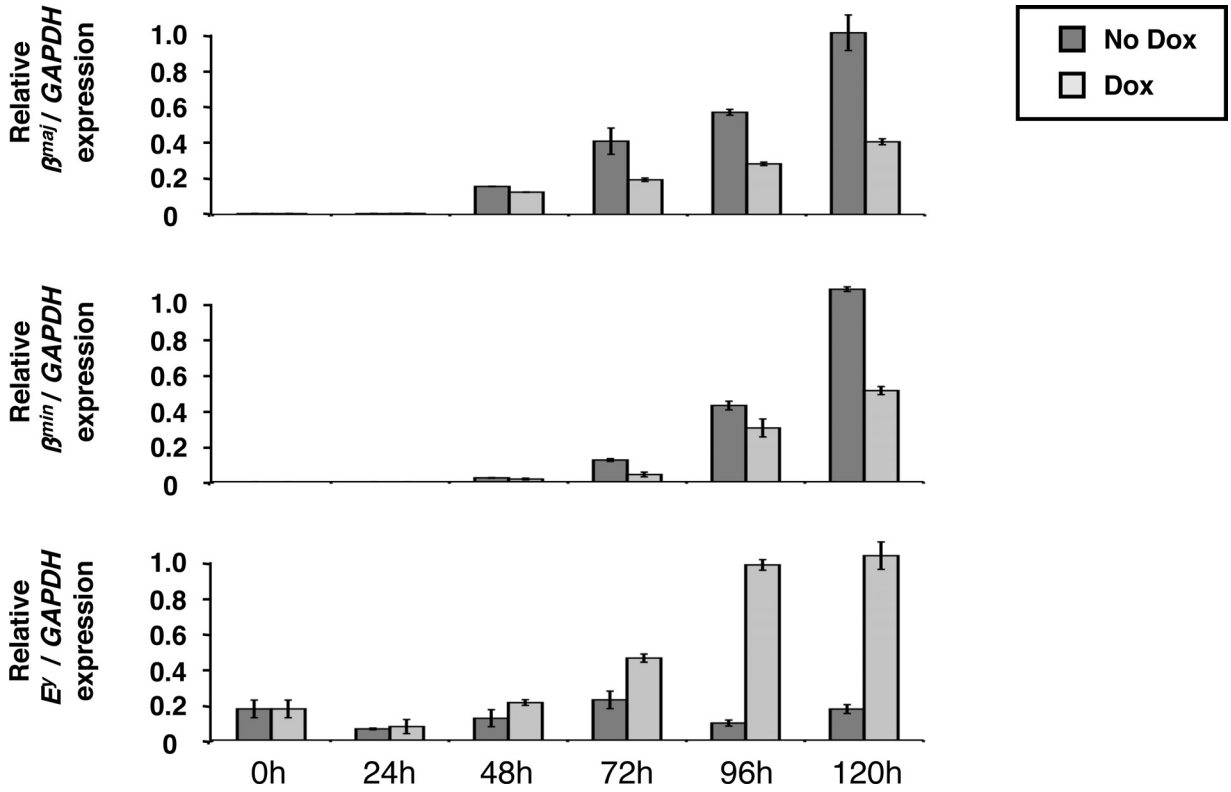

Fig. S3. During terminal differentiation of erythroid cells, G9a has a dual role in maintaining the embryonic *β-like globin* gene E^{γ} in a repressed state while simultaneously activating the adult *β-globin* genes β^{maj} *and* β^{min}. Time-course experiment whereby G9a KD and erythroid differentiation were induced simultaneously at time 0 via Dox and DMSO treatment. RNA was extracted each day for up to 5 days and analyzed by real-time RT-qPCR. Transcripts values are expressed relative to GAPDH with the highest ratio set to 1. Average values ± SD represent three independent experiments. Primers and probes sequences are provided in *SI Text*.

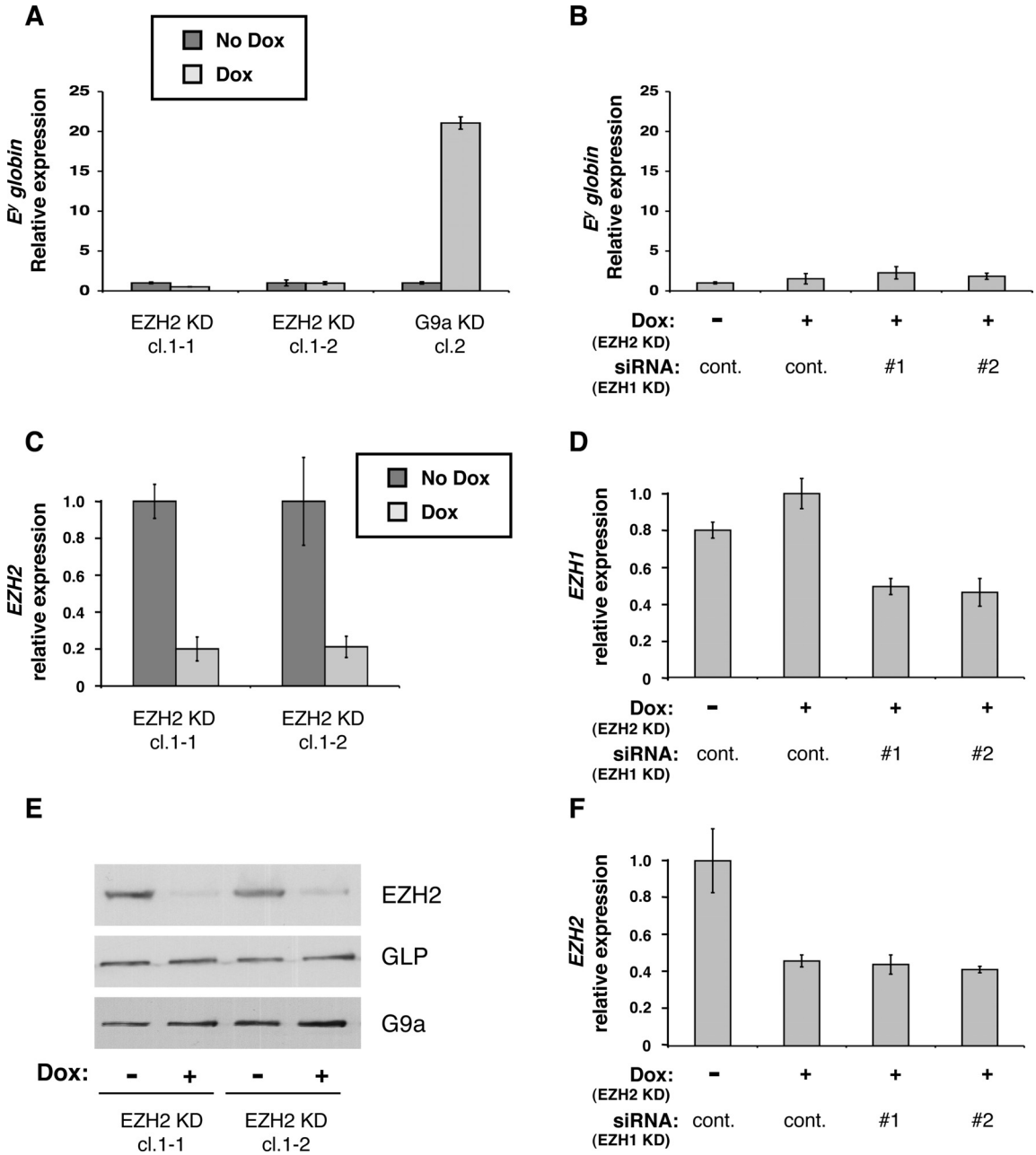

Fig. S4. EZH1/2 knockdown does not lead to reactivation of *Eγ globin* transcription in adult erythroid cells. (*A*) Knockdown (KD) of EZH2 (clones 1–1 and 1–2) and KD of G9a (clone 2) were induced by doxycyclin (Dox) incubation in differentiating MEL cells. Transcription of the embryonic *Eγ-globin* gene was assessed by real-time RT-qPCR after erythroid differentiation in EZH2 and G9a KD clones. *Eγ-globin* transcripts values are expressed relative to GAPDH with the no Dox ratio set to 1. (*B*) Anti-EZH1 siRNA sequences (#1 or #2) or a luciferase targeting control siRNA (cont.) were transfected into the EZH2 KD clone 1–2 16 h before Dox-induced EZH2 KD at a siRNA concentration of 100 nM using Oligofectamine reagent (Invitrogen) according to the manufacturers instructions. Transcription of the embryonic *Eγ-globin* gene was assessed by real-time RT-qPCR after erythroid differentiation. *Eγ-globin* transcripts values are expressed relative to GAPDH with the no Dox ratio set to 1. (*C*) KD of EZH2 (clones 1–1 and 1–2) was induced by Dox incubation in differentiating MEL cells. Transcription of the *Ezh2* gene was assessed by real-time RT-qPCR after erythroid differentiation. *Ezh2* transcripts values are expressed relative to GAPDH with the highest ratio set to 1. (*D*) Anti-EZH1 siRNA sequences (#1 or #2) or a luciferase targeting control siRNA (cont.) were transfected into the EZH2 KD clone 1–2 16 h before Dox-induced EZH2 KD at a siRNA concentration of 100 nM using Oligofectamine reagent (Invitrogen) according to the manufacturers instructions. Transcription of the *Ezh1* gene was assessed by real-time RT-qPCR after erythroid differentiation. *Ezh1* transcripts values are expressed relative to GAPDH with the highest ratio set to 1. (*E*) KD of EZH2 (clones 1–1 and 1–2) was induced by Dox incubation in differentiating MEL cells. EZH2 KD was assessed by Western blot. GLP and G9a were used as internal controls. (*F*) Anti-EZH1 siRNA sequences (#1 or #2) or a luciferase targeting control siRNA (cont.) were transfected into the EZH2 KD clone 1–2 16 h before Dox-induced EZH2 KD KD at a siRNA concentration of 100 nM using Oligofectamine reagent (Invitrogen) according to the manufacturers instructions. Transcription of the *Ezh2* gene was assessed by real-time RT-qPCR after erythroid differentiation. *Ezh2* transcripts values are expressed relative to GAPDH with the highest ratio set to 1. Average values ± SD represent three independent experiments. Primers and probes sequences are provided as *SI Text*.

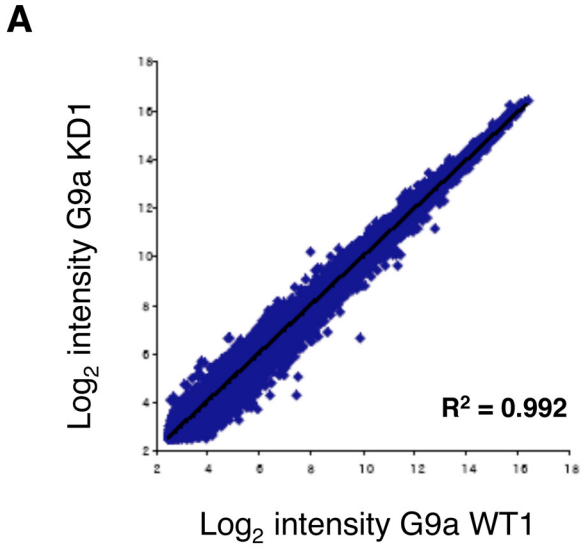

B

	R^2
WT1 *vs* KD1	0.992
WT2 *vs* KD2	0.995
WT3 *vs* KD3	0.994

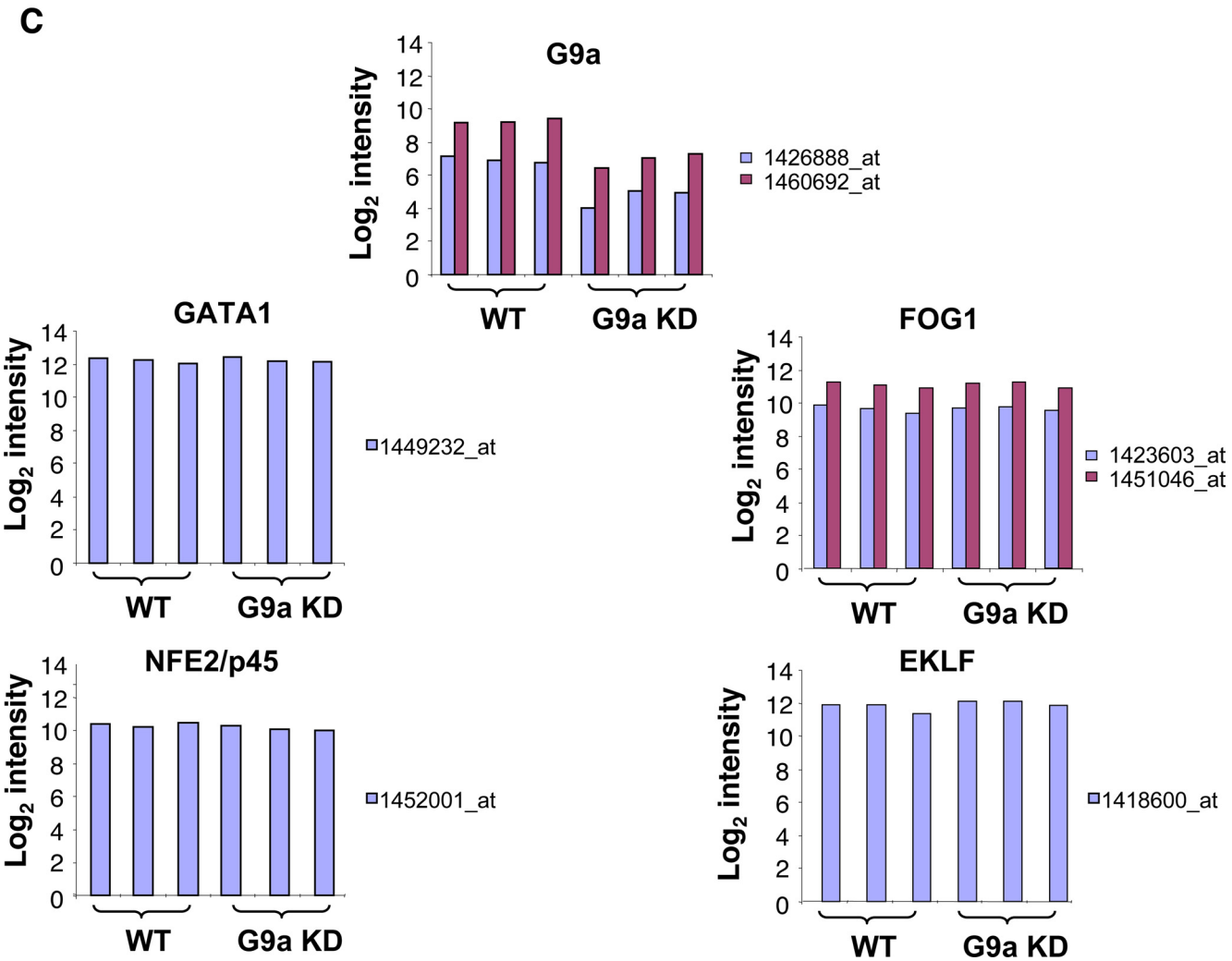

Fig. S5. G9a knockdown does not affect the overall gene expression profile of differentiated erythroid cells. (*A*) Normalized intensity values of wild-type (WT) vs. G9a knocked down (KD) Affymetrix Mouse Genome 430 2.0 gene expression microarray-replicate 1. (*B*) R^2 values of the three replicates. (*C*) Normalized intensity values for probe sets associated to G9a, GATA1, FOG1, NFE2/p45, and EKLF in triplicate microarray profiling. The indicated numbers correspond to the probes identification numbers on the array.

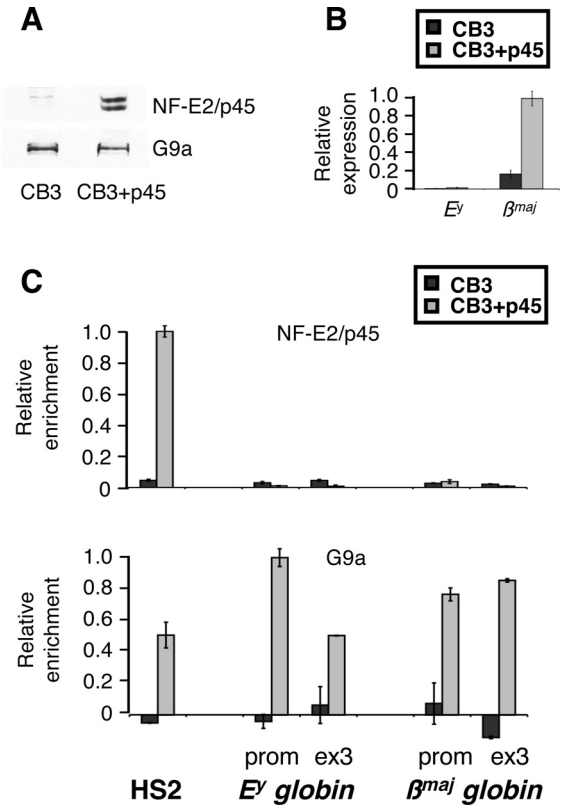

Fig. S6. NF-E2/p45-dependent binding of G9a to the β-globin locus. (*A*) Western blot of nuclear extracts prepared from the NF-E2/p45-null CB3 cell line (CB3) and from a rescued clone stably expressing an exogenous NF-E2/p45 protein (CB3+p45). (*B*) Transcription of the embryonic E^{γ} and adult β^{maj} globin genes was assessed by real-time RT-qPCR after erythroid differentiation in the CB3 and CB3+p45 cell lines. Transcripts values are expressed relative to GAPDH with the highest ratio set to 1. Average values ± SD represent three independent experiments. (*C*) ChIPs were performed after induction of differentiation in the CB3 and CB3+p45 cell lines to analyze the binding of NF-E2/p45 and G9a. ChIPs were revealed by qPCR using probes specific to the indicated genomic regions. Values are expressed as a function of the highest enrichment and represent average of at least two replicates ± SD.

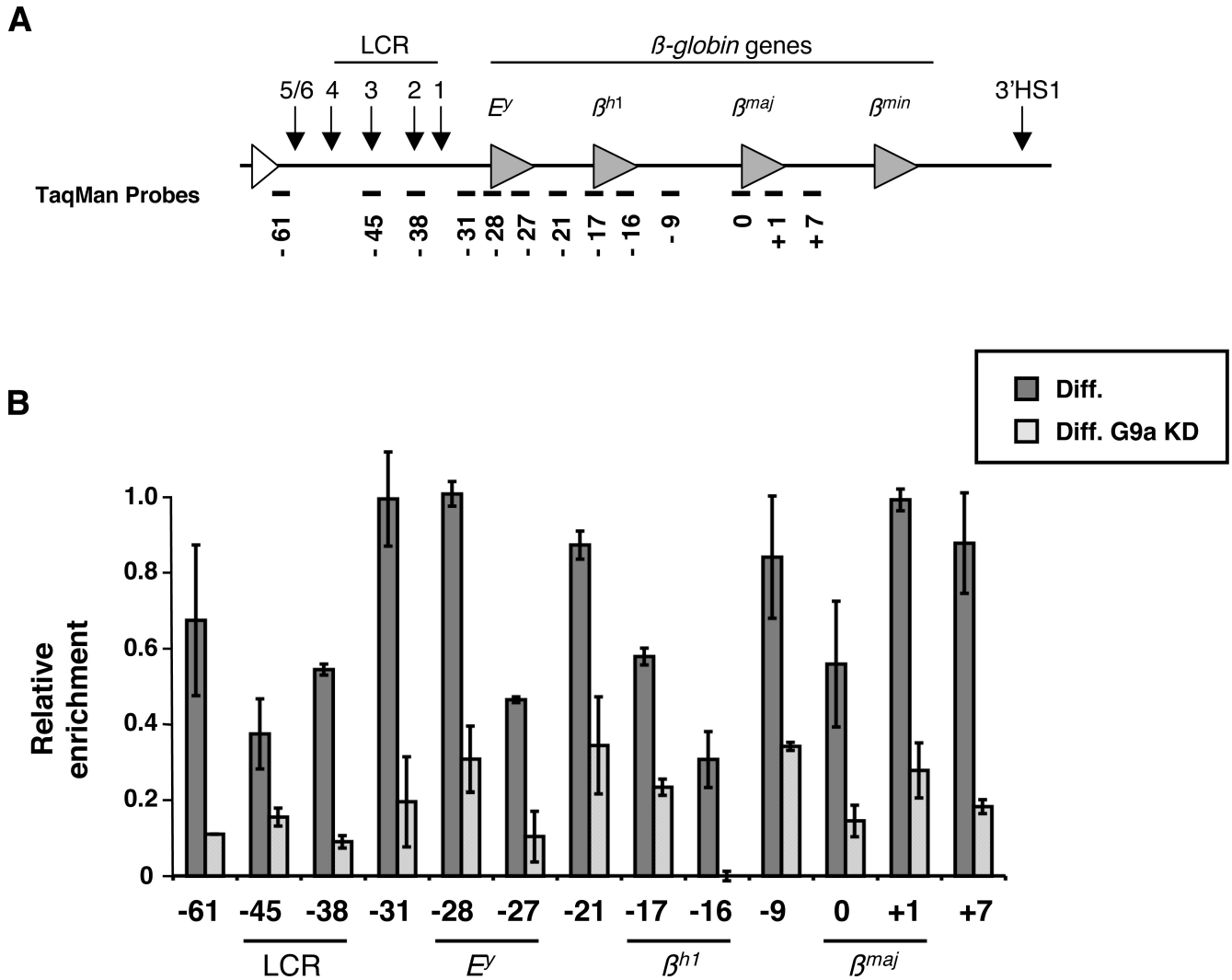

Fig. S7. G9a spreading along the β-globin locus in differentiated erythroid cells. (*A*) Schematic representation of the murine β-globin locus. Shaded triangles represent the *β-like globin* genes. The white triangle represents the inactive olfactory receptor gene. Vertical arrows represent DNase I hypersensitive sites (HSs). LCR indicates the Locus Control Region. Positions of the TaqMan probes used to reveal the ChIP by real-time qPCR are indicated in kb relative to the β^{maj} *globin* transcription start site (set to 0). (*B*) ChIP experiments were performed after induction of erythroid differentiation in G9a-depleted (Diff. G9a KD) versus normal (Diff.) MEL cells to analyze the binding of G9a. ChIPs were revealed by real-time qPCR using TaqMan probes indicated in (*A*). Values are expressed as a function of the highest enrichment and represent average of at least two replicates ± SD.

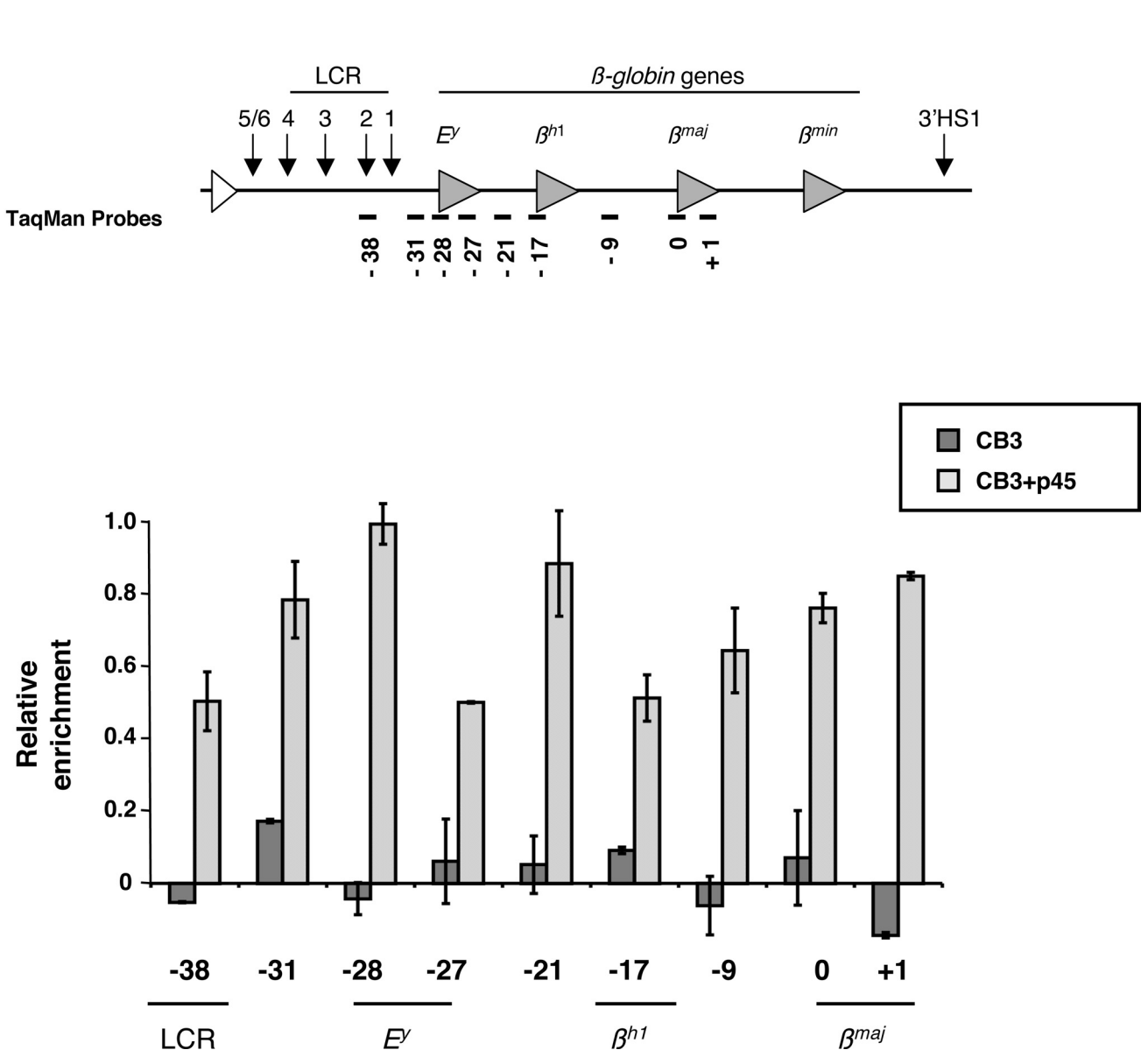

Fig. S8. G9a spreading along the β-globin locus in rescued CB3 cells. (*A*) Schematic representation of the murine β-globin locus. Shaded triangles represent the *β-like globin* genes. The white triangle represents the inactive olfactory receptor gene. Vertical arrows represent DNase I hypersensitive sites (HSs). LCR indicates the Locus Control Region. Positions of the TaqMan probes used to reveal the ChIP by real-time qPCR are indicated in kb relative to the β^{maj} *globin* transcription start site (set to 0). (*B*) ChIP experiments were performed after induction of erythroid differentiation in CB3 cells (CB3) and CB3 rescued by ectopic expression of p45 (CB3+p45) cells to analyze the binding of G9a. ChIPs were revealed by real-time PCR using TaqMan probes indicated in (*A*). Values are expressed as a function of the highest enrichment and represent average of at least two replicates ± SD.

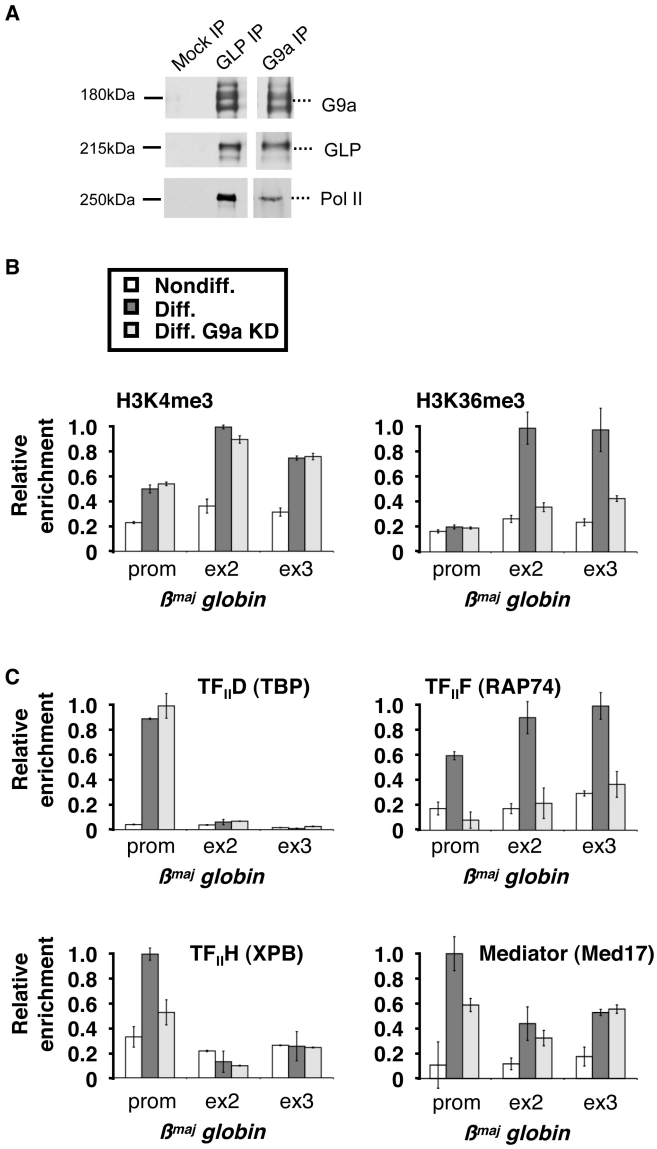

Fig. S9. G9a facilitates preinitiation complex (PIC) formation on the β^{maj} *globin* promoter independently of $TF_{II}D$ binding. (*A*) G9a interacts with the RNA polymerase II in nuclear extracts from erythroid cells. Western blot analysis of endogenous proteins immunoprecipitated from an erythroid nuclear extract via Abs against G9a and GLP. Mock IP with normal mouse IgG was used as a negative control. Abs used for Western blot are indicated on the right. (*B* and *C*) Chromatin immunoprecipitation (ChIP) experiments were performed before (Nondiff.) and after induction of erythroid differentiation in G9a-depleted (Diff. G9a KD) vs. normal (Diff.) MEL cells to analyze the enrichment of the H3K4me3 and H3K36me3 histone marks (*B*) and the binding of the TBP subunit of $TF_{II}D$, the RAP74 subunit of $TF_{II}F$, the XPB/p89 subunit of $TF_{II}H$, the Med17 subunit of Mediator (*C*). ChIPs were revealed by qPCR using TaqMan probes located within the promoter (prom), exon 2 (ex2), and exon 3 (ex3) of the E^{y} and β^{maj} *globin* genes as indicated. Values are expressed as a function of the highest enrichment and represent average of at least two replicates ± SD.